sciendo

DOI 10.2478/ama-2023-0010

acta mechanica et automatica, vol.17 no.1 (2023)

ASSESSMENT OF THE IMPACT OF WEAR AND TEAR OF RUBBER ELEMENTS IN TRACKED MECHANISM ON THE DYNAMIC LOADS OF HIGH-SPEED TRACKED VEHICLES

Piotr RYBAK*, Zdzisław HRYCIÓW*, Bogusław MICHAŁOWSKI*, Andrzej WIŚNIEWSKI*

*Faculty of Mechanical Engineering, Military University of Technology,
ul. gen. Sylwestra Kaliskiego 2, 00-908 Warszawa, Poland

piotr.rybak@wat.edu.pl, zdzislaw.hryciow@wat.edu.pl, boguslaw.michalowski@wat.edu.pl, wisniewski.andrzej@wat.edu.pl

received 12 October 2022, revised 25 November 2022, accepted 12 December 2022

Abstract: The operation of high-speed tracked vehicles takes place in difficult terrain conditions. Hence, to obtain a high operational reliability, the design or modernisation process must be precise and should consider even the slightest details. The article presents issues related to the problem of formulating vehicle models using partial models of flexible elements used in tracked mechanisms. Changes occurring in the shape and properties of elements such as track pads and roadwheel bandages as a consequence of operating conditions are presented. These changes are reflected in the presented elastic–damping characteristics of components of the crawler mechanism. Numerical studies have shown that deterioration of chassis suspension components after a significant mileage may increase dynamic loads (forces) acting on the running gear. Increased forces in the running gear naturally result in increased stresses in the road surface on which the vehicle is travelling, which can pose a danger (or excessive wear and tear) to road infrastructure components such as culverts, bridges and viaducts. In the literature, model tests of objects are carried out on models that represent new vehicles, and the characteristics of the adopted elements correspond to elements not affected by the process and operating conditions. Its influence should not be ignored in the design, testing and running of a special vehicle. The tracked mechanism, as running gear, is designed for special high-speed vehicles for off-road and off-road driving. Its design ensures high off-road traversability. The dynamic loads originating from off-road driving are superimposed on those generated by the engine, drive train and interaction of the tracks with the roadwheels, sprocket, idler and supporting tracks return rollers.

Key words: maintenance, tracked mechanism, rubber elements, roadwheel, high-speed tracked vehicle, characteristics, modelling

1. INTRODUCTION

The issues related to the tracked vehicle operation are described infrequently and to a rather limited extent in the literature. The authors of most publications consider and analyse the problems experienced in tracked vehicles in industrial applications, e.g., see literature [1, 2] or civil applications, e.g., see literature [3, 4]. In high-speed tracked vehicles (HSTVs), the issue is even more complex. It requires considering several factors that affect the effectiveness and safety of the execution of tasks. The operating conditions (terrain, climatic and meteorological conditions, and dust) are important, a general description of which is included in the literature [5]. An interesting approach to the problem, the influence of vehicle operating time, is presented in the literature [6], where the impact of wear and tear of suspension elements on the dynamic loads of the vehicle is considered. Research on prototype crawler pads of crawler track links is presented in the literature [7]. An analysis of the elastomeric cover pad wear and tear process has been shown to indicate its applicability in HSTVs. The issue of vehicle operational safety and dynamic loads affecting this safety is described in the literature [8, 9]. The papers [10, 11] present the results of numerical tests of vehicle models with crawler tracks that differ in the way the links are connected. Their effects have been analysed on the dynamic loads of the vehicle body when passing over road bumps. The paper [12] describes a model of the interaction of the track–wheel–terrain system and presents the results of model tests for two types of rubber continuous and metal multi-part crawler track belts. In the paper [13], the modelling process and results of load tests that occur on a crawler track with different ways to connect the links are presented. Dynamic forces acting on the vehicle running gear during driving focused on a crawler track were measured in experimental research, the results of which are presented in the paper [14]. The authors proposed and tested the concept of an active mechanism compensating force tension in the tracks. The research was carried out by using numerical analysis. The presented results point towards the reduction in crawler track dynamic tension magnitudes and stability improvement of the tracked mechanism. In the paper [15], a bench testing solution for the analysis of various load conditions of a rubber crawler track is presented. Particular attention has been focused on the forces and stresses that occur in it. The results obtained from the calculation have been compared with the experimental data, and good consistency has been obtained. The methods of calculation of the internal resistance of elements in tracked vehicles are considered in the paper [16]. Various models of roadwheel rolling resistance, rubber track belt bending and crawler track resistance are presented. The authors of the study concluded that the various existing models lead to inconsistent results, especially due to the lack of sufficient data in the case of conventional rubber tracks. In the paper [17], the double roadwheel resistance model including a

rubber double band is presented. Resistance is calculated as the total of roadwheel and track contact and the friction of wheel and track guide lugs. The model includes vertical and lateral loads of roadwheels, non-uniform pressure and relation of normal forces between the roadwheel and track guide lugs. As result of experimental and model investigations, solutions to reduce losses in running gear are proposed. The interaction of the elements of the crawler track mechanism with the ground using simplified substitute models has been presented in the papers [18, 19]. The calculation results have been validated with data from the literature and with the results obtained from detailed calculations of the models.

The crawler track mechanism is a running system in which the driving force generated by the engine, which causes the vehicle to move, is intermediated by the crawler tracks to the ground [20]. The high-speed tracked vehicle (HSTV) is a vehicle that develops a running speed of >25 km/h. With a gross vehicle weight of up to 70 t (tonne), such vehicles can reach speeds of up to 75 km/h on paved roads and up to 55 km/h off-road. Such conditions result in increasingly complex dynamic loads of high intensity and random varying parameters.

It is usually assumed that the elastic and damping properties of suspension elements remain essentially unchanged in the lifetime of the track running gear system, whereas the elastic and damping properties of rubber elements of crawler track mechanisms change quite significantly due to wear and tear, mechanical damage, temperature effects and the operating environment. The literature presents results mainly obtained from model tests of new vehicles. For example, the papers [21–23] present models and results of analysis of the interaction of crawler tracks with different types of ground. On the contrary, the paper [24] analyses the effect of the arrangement of shock absorbers on the dynamic loads acting on the tracked vehicle. Some parameters or characteristics are assumed to be invariant during the operating process, while others are ignored. The results of numerical investigations of the 2S1 tracked mechanism with modified suspension are presented in the paper [25]. Torsion bars are replaced with hyperbolic springs. As the result of the proposed modifications improved the stability of the vehicle and reduced the interior and the exterior volume of the vehicle suspension. In the paper [26], a vehicle has been analysed in which the stiffness of the new rubber bandages of the roadwheels has been included, neglecting their damping. In the paper [23, 27], a tracked vehicle model has been used for simulation studies to assess the effects of the terrain geometry, soil characteristics and speed on vehicle performance.

Articles considering the impact of ageing wear and tear of rubber elements in the running gear of tracked vehicles on dynamic loads of HSTVs, such as medium tanks, and its impact on the environment are uncommon. This applies particularly to rubber bands on roadwheels and rubber pads on tracks.

It can be considered that the studies carried out do not take account of the changes in the properties of the elements of the crawler track mechanism of the vehicles, especially in those elements where rubber is used. These changes are due to the distance travelled, speed of travel, type of ground, weather conditions and material ageing. It can be assumed that the material used in this study fills the gap well in this field area.

The genesis of the undertaken topic is the process of modernisation of combat vehicles. It originates in the necessity of improvement of the safety of the crew, leading to an increase in the sprung mass and engine horsepower. As a consequence, roadwheel rolling resistance and dynamic loads or running gear increase.

This study aims to evaluate the effect of wear and tear of rubber elements in the running gear occurring during typical vehicle operation conditions on the change in dynamic loads acting on the vehicle chassis, hull and crew.

2. OPERATING LOADS OF VEHICLE RUNNING GEAR

The natural operating conditions of the HSTV are shown in Fig. 1. The main loads on the crawler track mechanism and the intensity of wear of its elements depend, among other things, on the mass of the vehicle m_b [kg], time of use t [h], running speed v [m/s], steering angular velocity ω [1/s], temperature Δt [°C], pre-tension of crawler tracks P_w [N], height of ground bumps h [m], their distribution and length l_p [m], type of ground (sand, clay, rocks, etc.) f_{gr} and physical properties of construction materials *WM*. Thus, its durability T is mainly a function of factors such as in Eq. (1):

$$T = f(m_b, t, y, v, \omega, \Delta t, P_w, l_p, f_{gr}, WM) \tag{1}$$

The design pre-tension of the P_W crawler track belt is given by Eq. (2):

$$P_W = \frac{\rho \cdot g \cdot l^2}{8 \cdot f} \tag{2}$$

where ρ is the unit mass of the crawler track [kg/m], g is the acceleration due to gravity [m/s^2], l is the length of the freely hanging section of the crawler track [m] and f is the deflection arrow [m]. The pre-tension of the crawler track should meet the following condition: $f_{min} \leq f \leq f_{max}$ (where f_{min} is the deflection arrow at the minimum tension and f_{max} is the deflection arrow at the maximum tension).

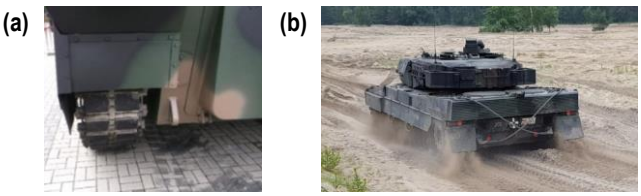

Fig. 1. Natural conditions for the movement of special vehicles: (a) cornering on a paved road and (b) unsurfaced road

Only the tracked vehicle contains a road that can be assumed to have an infinite length. Crawler track belts are unfolded in front of roadwheels, smoothing out the bumps to overcome. After the last wheel has passed, they are taken up from the ground, rewound and unfolded again. The large load-bearing surface of the crawler tracks (Fig. 2) provides vehicles considerable weight with a low average unit pressure ps Eq. (3), as follows:

$$p_s = \frac{G}{2 \cdot F} = \frac{m_b \cdot g}{2 \cdot L_0 \cdot b} \tag{3}$$

where G is the force of gravity of the vehicle, F is the area of the lower track branches, L_0 is the length of contact between the lower track and the ground, b is the width of the track and g is gravitational acceleration.

Contemporary HSTVs up to 40 t have an average unit pressure on the deformable ground of p_s = (40–70) kPa. The average unit pressure of vehicles >40 t is in the range p_S = (75–100) kPa. The tactical and technical requirements for HSTVs >40 t impose a

DOI 10.2478/ama-2023-0010

prerequisite that average pressures should not exceed $p_s \leq 85$ kPa. For wheeled vehicles (including multi-axle vehicles), the pressure value is much higher and is in the range p_s = (170–350) kPa [8]. An increase in specific pressures increases the ground resistance force F_{gr} Eq. (4), as follows:

$$F_{gr} = Z \cdot f_{gr} = G \cdot f_{gr} \cdot \cos\alpha \tag{4}$$

where f_{gr} is the ground resistance coefficient, N is the normal reaction and α is the road slope angle.

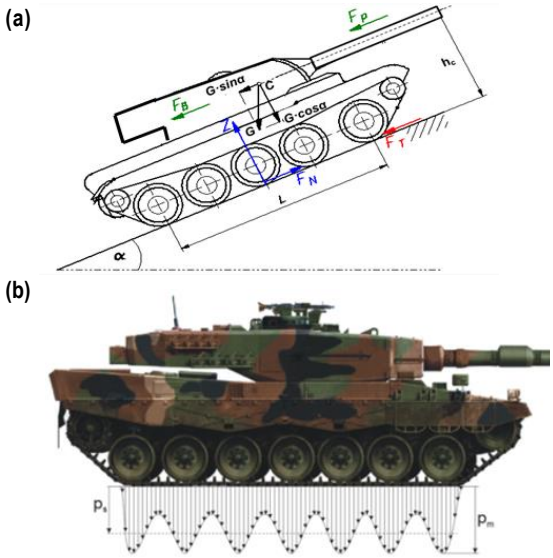

Fig. 2. Diagram showing the interaction of the crawler track mechanism with the ground: (a) diagram of the forces acting on the HSTV and (b) distribution of ground pressures: pm – maximum value, ps – average value

The pressure value p_s combined with the high ground adhesion F_φ Eq. (5) makes it much easier for tracked vehicles to navigate in difficult terrain conditions (φ is the coefficient of adhesion of crawler tracks to the ground).

$$F_\varphi = 0.65 \cdot G \cdot \varphi \tag{5}$$

Some of the data and results of the studies and analyses, due to the status of the vehicles analysed, are characterised by a certain sensitivity value. It should be assumed that they have qualitative, rather than quantitative, qualities.

3. RUBBER ELEMENTS IN THE CRAWLER TRACK RUNNING MECHANISM AND ITS EXTERNAL FACTORS OF WEAR

In motor vehicles, rubber elements (with different shapes, material compositions, manufacturing methods and characteristics) are used extensively, whereas in HSTVs, some of the rubber elements are quite different from the typical rubber elements and have a special role in the operating process. Those are integral parts of the assemblies and elements of the crawler track mechanism subjected to complex dynamic loads in the surrounding environment. Some of the structural assemblies of the crawler track mechanism that use rubber with given properties, shape and geometry are shown in Figs. 3–8. Fig. 3 shows a roadwheel with a vulcanised rubber band of the appropriate thickness and width (these parameters depend on the weight and inertia of the vehicle, the number of roadwheels and the model of interaction of the crawler track with the ground). The use of external rubber bandages enables:

- a reduction in the amount of heat liberated by the friction of the rubber band against the track links compared to pure steel wheels;
- a reduction in the dynamic loads acting on the vehicle hull and crew;
- a reduction in the noise level during driving; and
- a reduction in the amount of heat released during the friction of the rubber band against the crawler track belts compared to steel-rimmed wheels featuring internal shock absorption.

Fig. 4 shows sections of the crawler track belts and links used in HSTVs, with a crawler track of the hinge type (Fig. 4a) and a crawler track of the link type (Fig. 4b).

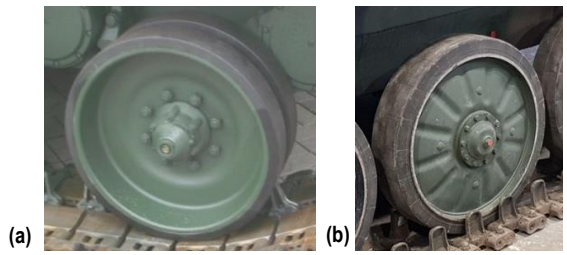

Fig. 3. Roadwheel with an outer rubber band: (a) double outer rubber band and (b) single outer rubber band

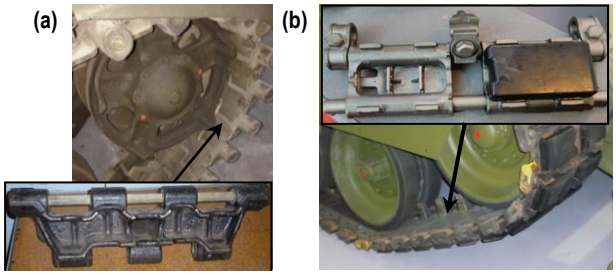

Fig. 4. Hinge (a) and link (b) types of crawler tracks

The links of the crawler track of the hinge type, with a weight of up to 16 kg, are connected by a single pin (Fig. 4a), whereas the links of the crawler track of the link type, with a mass of up to 24 kg, are connected by two pins (Fig. 4b). The links rotate relative to each other by deforming the rubber bushings in a torsional manner, forming the so-called closed joint. To reduce the load on the bushings and reduce the energy loss while driving, the links are connected at an appropriate angle when assembled (angle α in Fig. 5).

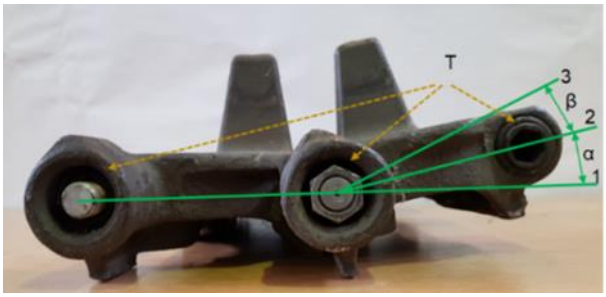

Fig. 5. Crawler track links with a rubber and metal joint: T – rubber-metal bushings, 1 – line parallel to the ground surface, 2 – line of zero torsional stress, 3 – line of maximum torsional stress, α – mounting angle of links, β – angle of maximum relative rotation of links

In the HSTV crawler tracks, interchangeable link cover pads of the crawler track are used (Fig. 6), which can be fixed in an elastic holder (Fig. 6a) or with a screw (Fig. 6b).

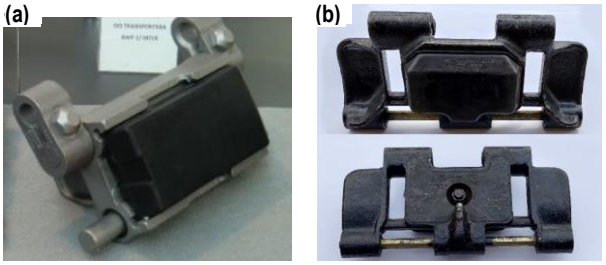

Fig. 6. Link cover pads of the HSTV crawler tracks fixed: (a) pressed into guides and (b) screwed into the socket

Rubber cover pads of crawler tracks contribute to the ability to be driven on public roads (by reducing pavement loads) as follows: a reduction in the amount of heat released when the cover plate is in friction with the ground compared to a metal crawler track, a reduction in vehicle slip-on paved surfaces, a reduction in the noise level when driving, a reduction in dynamic loads when driving off-road, an increase in grip on hard rough pavement and a reduction in grip on soft ground. On vehicles where roadwheels have a reduced thickness band in addition to cover plates, rubber cushions may be used on the inner surfaces of the links, as shown in Fig. 7.

Fig. 7. Rubber cushions on the inner surface of the links of crawler tracks

During the operation of HSTVs, insufficient resistance of some elements of the crawler track mechanisms to complex operating loads can be observed. This affects the durability and reliability not only of the crawler track mechanism but also of other vehicle units and systems. The aforementioned applies to both the cover pads of the crawler track links, which have a specified odometer reading of 1,000–1,500 km, and the bandages of roadwheel, whose wear and tear and failure rate depend on the intensity of use, dynamic loads, ambient and operating temperatures. Examples of damage to bandages and cover plates are shown in Figs. 8a and 9. When driving on a hard, rough road surface:

- rubber track pad plates are subject to abrasive wear and tear during cornering (Fig. 1a), and the weight of the links and crawler tracks may change (also by tearing out rubber fragments – Fig. 8b);
- rubber track pads plate, as a result of wear and tear, can cause a reduction in the thickness of the damping layer and an increase in the noise level during dynamic driving may occur (the cause for this phenomenon is the uneven weight distribution in the link. In the link, different inertial forces act on the pins, drive wheels, directional wheels, roadwheels and support rollers); and
- rubber track pad plates can cause a risk of loss of stability at high speeds in curvilinear motion.

On deformable ground:

- rubber cover pads have an impact on running resistance, depending on the shape and geometry of the link and the cover pads and their degree of wear and tear;
- during dynamic driving and cornering, the track is at risk of dropping or tipping over on the dry, turf-covered ground.

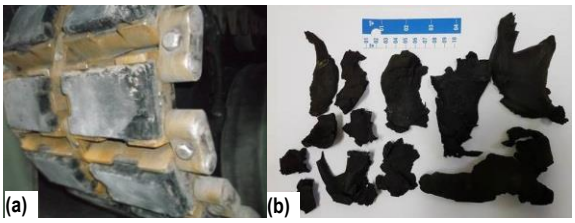

Fig. 8. Rubber cover plates: (a) with varying degree of wear and tear and (b) torn out rubber pad fragments

A confirmation of the considerable load on the links of crawler tracks and their wear during an interaction with the ground is shown in Fig. 9, where Fig. 9a shows a link of a new metal crawler track, while Fig. 9b after greater mileage. The abrasive wear of the ground grapples is visible.

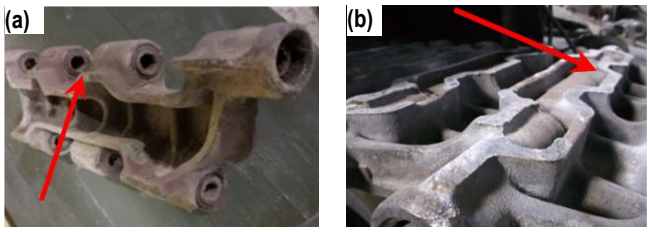

Fig. 9. Working surfaces of metal ground gripples of links. (a) new link and (b) used link

An important element that affects the efficiency and durability of crawler track belts is the link joints. The introduction of rubber and metal joints has, irrespective of the type of crawler track, eliminated the possibility of direct engagement between pins and link lugs in highly abrasive environments.

The rubber bandages of the roadwheels carry complex dynamic loads in the radial, circumferential and transverse directions when the vehicle is in motion. Roadwheels may also be exposed to external mechanical sources such as stones, debris and rocks. This process also generates thermal loads, which can have a significant impact on the elastic properties of rubber. The result of the aforementioned impacts is damage to the bandages. Examples of the most common damage cases are shown in Fig. 10. The running conditions of special HSTVs, in military applications, pose some challenges to vehicle designers and manufacturers. The rubber used for the structural elements of the crawler track mechanism must meet the assumed requirements and be characterised by appropriate properties, especially within scope of:

- high resistance to mechanical stress (compression, tension, impact, chipping, tearing);
- good energy absorption (vibro-insulating properties) to reduce dynamic loads on the vehicle hull and crew;
- high abrasion resistance;
- high adhesion to metals (vulcanising properties);

– high thermal resistance (non-combustible or self-extinguishing); and
– good thermal conductivity, heat dissipation into the superstructure (load-bearing wheel rim, base of cover plate, etc.) and environmental resistance (ageing, exposure to operating fluids).

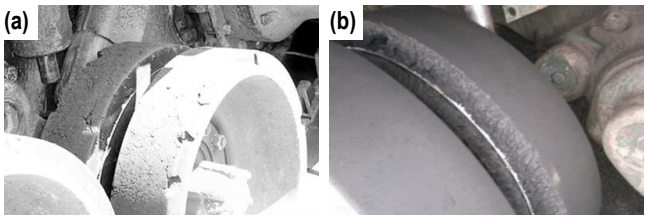

Fig. 10. Damage to the rubber bands of the load-bearing wheels: (a) abrasive and mechanical wear and (b) interaction of the track guide ridges and devulcanisation of the bandage from the rim

The change in the elastic and damping (ED-RP) properties of the rubber elements of the crawler track mechanism after a significant mileage is the result of the impact of a number of factors. The main factors are summarised in the following Eq. (6):

$$ED - RP = f(WM, shape\ (a\ x\ b\ x\ c), t_e, v, P_{ks}, P_w, P_k, P_o, \sigma_z, \Delta t) \quad (6)$$

where *WM* is the physical properties of the material, *a* x *b* x *c* is the *(length x width x height)* dimensions of cover plate [m], t_e is the time of use [h], *s* is the mileage [km], P_{ks} is the static load [kN], P_k is the crawler track tension from driving force [kN], P_k is the crawler track tension resulting from centrifugal force [kN], σ_z is stresses and Δt is the temperature increment.

4. METHODOLOGY

4.1. Experimental setup

The models for testing should be built on the actual characteristics of elements and also with an observation of changes occurring during day-to-day running. To identify the relevant parameters of selected rubber elements, bench tests have been conducted. The tests were carried out on an Instron 8802 machine. Each of the test objects was subjected to deflection from 5 mm to 14 mm, with a frequency in the range of 0.1–2 Hz. For each variant, 10 load cycles have been carried out. Fig. 11a shows the test bench while testing a sample of a roadwheel with a rubber bandage, and Fig. 11b shows the test bench with a rubber pad during axial compression. The initial deflection of the rubber pad was 7 mm.

The stiffness (*k*) of the elements under test is determined from the elastic characteristics for the static equilibrium position, from the following Eq. (7):

$$k = \frac{\Delta P}{\Delta f} \quad (7)$$

or determined by Young's modulus of the sample material of the element, obtained from the following Eq. (8) [28]:

$$k = \frac{E \cdot A}{h} \quad (8)$$

where *P* is the element load [kN], f is the displacement [mm], E is the determined Young's modulus [MPa], A is the surface area of the sample [mm^2] and h is the height of the sample [mm].

The dispersion coefficient ψ is determined from the following Eq. (9):

$$\Psi = \frac{\Delta W}{W} \quad (9)$$

where ΔW is the value of energy dispersed during one vibration cycle [J] and W is the value of energy supplied to the system during this vibration cycle [J].

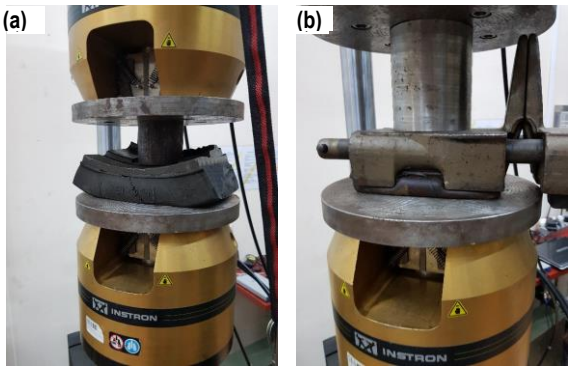

Fig. 11. Bench testing of elements of crawler track mechanism: (a) a sample of roadwheel with rubber bandage and (b) a rubber pad

4.2. Numerical model

Depending on the purpose of the study, vehicle models are characterised by varying degrees of complexity. These can be discrete models with one, two and a finite number of degrees of freedom or models developed and analysed by FEM [29]. Partial models can be used to analyse complex dynamic objects such as HSTVs, as demonstrated in the paper [30].

Fig. 12 shows a model of the high-speed tracked vehicle adopted for the analysis. The relevant partial models of the susceptible elements of the crawler track mechanism have been distinguished in it.

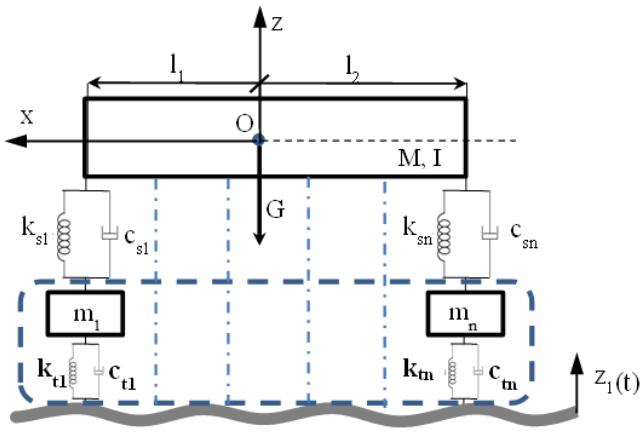

Fig. 12. HSTV model: M – body mass, I – body moment of inertia, G – gravity, k_{s1}, ..., k_{sn} – spring stiffness of the suspension, c_{s1}, ..., c_{sn} – suspension damping, k_{t1}, ..., k_{tn} – stiffness, c_{t1}, ..., c_{tn} – damping of the rubber elements of the crawler track mechanism, and n – number of roadwheels at one side

The equation of motion of the vehicle is given by the following Eq. (10):

$$\boldsymbol{M}\ddot{q} + \boldsymbol{C}\dot{q} + \boldsymbol{K}q = \boldsymbol{F}\Psi = \frac{\Delta W}{W} \tag{10}$$

where *M* is the diagonal inertia matrix of the system, q is the generalised displacement vector, *C* is the damping matrix, *K* is the stiffness matrix and *F* is the generalised force vector resulting from the kinematic excitations acting on the wheels.

Numerical investigations were performed with the original finite element code. In the investigation, there were 18 degrees of freedom, including vertical displacement of wheels Eq. (12), the hull and the driver seat Eq. (2), and rotations along the longitudinal (x) and traversal (y) axes of the vehicle hull Eq. (2) and the driver seat Eq. (2). The model includes non-linear sprung and damping characteristics of vehicle suspension. The test object has been the hypothetical HSTV with a mass of 42 t, the moment of inertia I_x=92,000 kg/m^2 and I_y=190,000 kg/m^2 based on the undercarriage of a medium-sized tank, and running speed of 30 km/h on a non-deformable road with a single obstacle in the form of two road bumps, first in the shape of (1-cos) function (obstacle A) and second in form of a triangular prism shape (obstacle B).

The shape of the first obstacle is given by Eq. (11), while the second by Eq. (12):

$$z(t) = \begin{cases} \frac{h}{2} \cdot \left(1 - cos \cdot \left(\frac{2 \cdot \pi \cdot V \cdot t}{L_b}\right)\right), & t \le \frac{L_b}{V} \\ 0, & t > \frac{L_b}{V} \end{cases} \tag{11}$$

where h is the obstacle height [m], V is the driving speed [m/s] and L_b is the obstacle length [m].

$$z(t) = \begin{cases} \frac{h \cdot \mathrm{V} \cdot \mathrm{t}}{L_p}, & t \le \frac{L_p}{V} \\ \frac{h}{L_p}(2 \cdot \mathrm{L} - \mathrm{V} \cdot \mathrm{t}), & \frac{L_p}{V} < t \le \frac{2 \cdot L_p}{V} \\ 0, & t > \frac{2 \cdot L_p}{V} \end{cases} \tag{12}$$

where L_p is the half of total obstacle length [m].

Both had a height of 0.15 m and a length of 1 m. Model studies can also be carried out for other obstacle profiles such as threshold, sinusoidal track also combined with kinematic shape with pseudo-random distribution (various quality road).

5. RESEARCH RESULTS

5.1. Experimental investigation

Fig. 13 shows the results of measurements not subjected to additional processing steps. The graph also shows the deflection spike near zero load force, caused by the detachment of the rubber pad from the stand base. The stiffness characteristic presented in Fig. 14 is not suitable for implementation in the numerical investigation. One cycle was selected from the recorded trial, then the approximations for force load and unload phases were determined with an average curve, and an area of the hysteresis loop corresponding to the dissipation energy was determined.

The aforementioned procedure was applied both for rubber pads and a section of roadwheel with a rubber bandage. The numerical study assumes the implementation of the running system as a substitute model. The rubber band works in series with the rubber pad in the vehicle running system. Fig. 15 shows individual characteristics, where blue denotes a new rubber pad (RP1), green denotes a new rubber band (RB) and resultant characteristic and yellow denotes a series connection (RP1 and RB). Fig. 16 shows individual characteristics, where blue denotes a used rubber pad (RP2), green denotes a new rubber band (RB) and resultant characteristic, and yellow denotes a series connection (RP2 and RB).

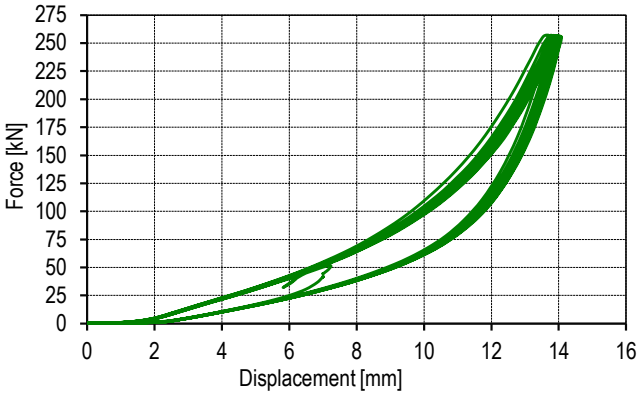

Fig. 13. Stiffness characteristic for the new rubber pad consisting of ten cycles

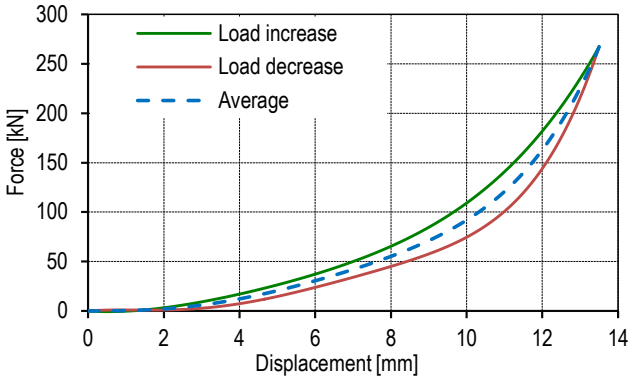

Fig. 14. Processed stiffness characteristic: force load (green line), force unload (brown line) and suitable for numerical investigation form visible as a dashed line

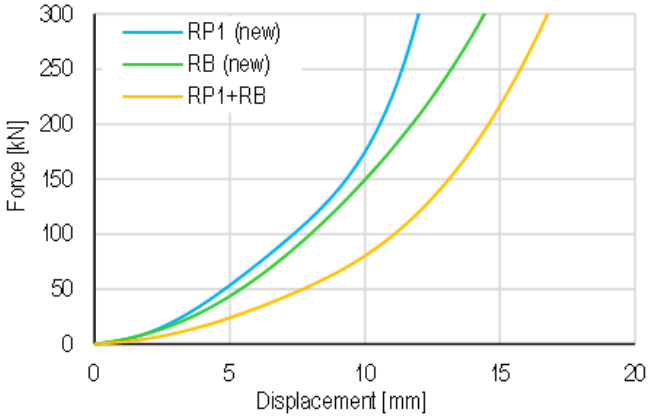

Fig. 15. Approximated stiffness characteristics: blue line – new rubber pad, green – new rubber band, yellow – resultant characteristic

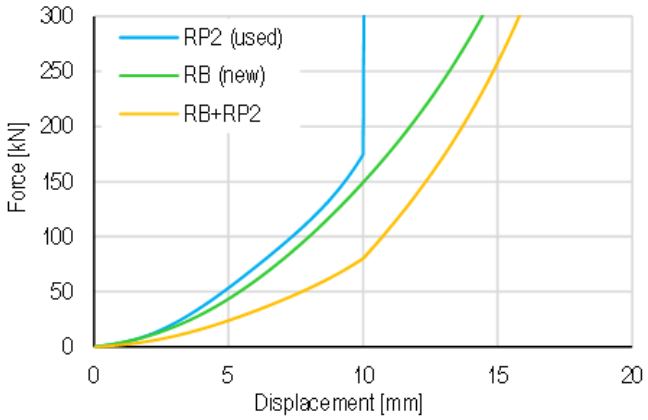

Fig. 16. Approximated stiffness characteristics: blue line – used rubber pad, green – new rubber band, yellow – resultant characteristic

5.2. Model research

Model tests have several advantages: they are non-destructive, enable a multivariate analysis in a short time, do not require a large investment and are safe. Depending on the specific characteristics of the elastic and damping elements present in the crawler track mechanism, it is possible to determine, at each stage of operation, the loads on the hull as well as the driver, the dynamic reactions of the load-bearing wheels and the deflection of the rubber bandage, allowing the determination of ground loads. Examples of the dynamic load patterns from the tests for the rubber elements analysed – new and after the run – are shown in Figs. 17 and 18.

The main part of Fig. 17a shows the acceleration waveforms of six roadwheels when passing a single A-type obstacle for a new rubber band and new rubber pad configuration (conf. I). Sections of the graph enclosed by a dashed red line shows acceleration waveforms of peak areas for the new rubber band and used rubber pad configuration (conf. II). In case of conf. I, high acceleration values are observed when the first, second and sixth roadwheels are running into an obstacle. Deceleration values occurring are similar levels except for the first roadwheel (lowest deceleration value of 241 m/s^2) and sixth roadwheel (highest deceleration value of 255 m/s^2). In case of conf. II, waveform patterns are similar. The highest acceleration values are observed for the first, second and sixth roadwheels, higher by an average of around 7.2%. In the case of deceleration values, extreme values were observed for the first and sixth roadwheels. The lowest deceleration value was observed for the first roadwheel (212 m/s^2), while the highest deceleration value was observed for the sixth roadwheel (239 m/s^2). This is equivalent to a change of 12% and 6.3%. Tab. 1 summarises the detailed acceleration, and deceleration values and their percentages for the compared configurations, respectively.

The main part of Fig. 17b shows waveforms of forces transmitted by six roadwheels when passing a single A-type obstacle for a new rubber band and new rubber pad configuration (conf. I). Sections of the graph enclosed by a dashed red line shows force waveform peak areas for a new rubber band and used rubber pad configuration (conf. II). In case of conf. I, the highest force values are observed when the first, second and sixth roadwheels are running into an obstacle. The maximum force value is ≈108 kN. For the same wheels, a reduction in the transmitted force to zero is observed. This is equivalent to the condition in which the roadwheels become detached from the road surface. In case of conf. II, waveform patterns are similar. The highest values of force transmission are observed for the first, second and sixth roadwheels, higher by an average of around 3.3%. For the first, second and sixth roadwheels, detachment from surface was also observed. Tab. 2 summarises the detailed extreme force values and their percentages for the compared configurations.

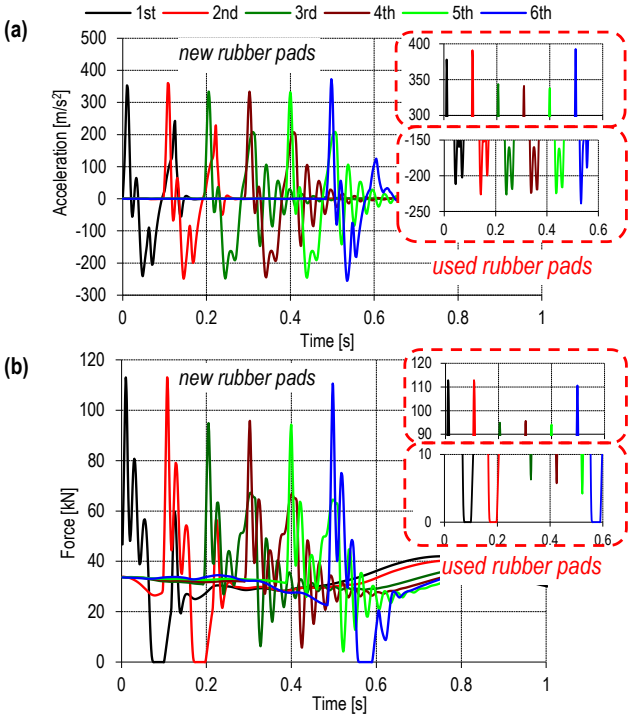

Fig. 17. Vertical acceleration waveforms of roadwheels passing a single A-type obstacle for conf. I (a) and conf. II in section of graph enclosed by a dashed red line. Force exerted on roadwheels for conf. I (b) and conf. II in section of graph enclosed by dashed red line

Tab. 1. Roadwheel vertical acceleration peak values and relative differences for tested configurations: a new rubber pad[1] and worn-out rubber pad[2]

Roadwheel number	Acceleration [m/s^2]				|Difference| [%]	
	max[1]	max[2]	min[1]	min[2]		
1st	352	378	–241	–212	7.4	12.0
2nd	360	391	–248	–226	8.6	8.9
3rd	334	344	–248	–226	3.0	8.9
4th	334	341	–245	–224	2.1	8.6
5th	332	336	–246	–224	1.2	8.9
6th	372	393	–255	–239	5.6	6.3

[1]conf. I: new rubber band, new rubber pad.
[2]conf. II: new rubber band, used rubber pad

Tab. 3 summarises the data covering the maximum and minimum values of rubber deflection (for the equivalent stiffness characteristics, the determination is shown in the fourth section). Tab. 3 confirms the detachment of the first, second and sixth roadwheels in both scenarios. The highest deflection values are observed for these roadwheels. In the case of the third and fourth roadwheels, both minimum and maximum deflection values are

similar. In the case of the fifth roadwheel, smaller deflection peak values were observed (0.5 mm). The two tested configurations showed an impact of rubber pad wear on the working range (deflection). In the case of the second, third and fourth roadwheels, a minimum deflection value increase for conf. II about 42.1% was observed. A maximum deflection change of values is an order of magnitude lower and decreased by about 1%. A greater change was observed for the first, second and sixth roadwheels, a decrease by an average of 5%.

The condition of the rubber elements has an impact on loads acting on roadwheels and suspensions but did not significantly affect the loads acting on the vehicle hull and the driver.

Tab. 2. Peak values and relative differences of force exerted on roadwheel for tested configurations: a new rubber pad[1] and worn-out rubber pad[2]

Roadwheel number	1st	2nd	3rd	4th	5th	6th
F_{max}[1] [kN]	108	108	93	94.2	93.2	107
F_{max}[2] [kN]	113	113	94.9	95.7	94.1	111
|Difference| [%]	4.63	4.63	2.04	1.59	0.97	3.74
F_{max}[1] [kN]	0*	0*	5.63	5.00	3.48	0*
F_{max}[2] [kN]	0*	0*	6.29	5.74	4.20	0*
|Difference| [%]	N.A.	N.A.	11.7	14.8	20.7	N.A.

[1]conf. I: new rubber band, new rubber pad.
[2]conf. II: new rubber band, used rubber pad
*Detachment of the roadwheel from the ground.
N.A. – not applicable.

Tab. 3. Rubber deflection peak values and relative differences for tested configurations: a new rubber pad[1] and worn-out rubber pad[2]

Roadwheel number	Deflection [mm]				|Difference| [%]	
	max[1]	max[2]	min[1]	min[2]	min	max
1st	0*	0*	–11.4	–11.0	N.A.	3.86
2nd	0*	0*	–11.4	–11.0	N.A.	4.18
3rd	–2.1	–2.9	–10.5	–10.4	38.1	0.91
4th	–2.0	–2.7	–10.6	–10.5	35.0	1.23
5th	–1.5	–2.3	–10.6	–10.4	53.3	1.39
6th	0*	0*	–11.2	–11.0	N.A.	2.52

[1]conf. I: new rubber band, new rubber pad.
[2]conf. II: new rubber band, used rubber pad
*Undeformed rubber (detachment of roadwheel from the ground).
N.A. – not applicable.

The main part of Fig. 18a shows acceleration waveforms of six roadwheels when passing a single B-type obstacle for a new rubber band and new rubber pad configuration (conf. I). Sections of the graph enclosed by a dashed red line shows acceleration waveform peak areas for a new rubber band and used rubber pad configuration (conf. II). In case of conf. I, significantly higher acceleration values are observed for the third, fourth and sixth roadwheels overcoming an obstacle.

Deceleration values are similar, except for the first (lowest deceleration value of 476 m/s^2) and second roadwheels (highest deceleration value of 461 m/s^2). In case of conf. II, waveform patterns are similar. The highest acceleration values are observed for the third, fourth and fifth roadwheels, higher by an average of around 1.9%. In the case of deceleration values, extreme values were observed for the first and second roadwheels. The lowest deceleration value was observed for the fifth roadwheel (416 m/s^2), while the highest deceleration value was observed for the first roadwheel (472 m/s^2). This is equivalent to a change of 1.96% and 0.84%. Tab. 4 summarises the detailed acceleration and deceleration values and their percentages for the compared configurations. The main part of Fig. 18b shows waveforms of forces transmitted by six roadwheels when passing a single B-type obstacle for a new rubber band and new rubber pad configuration (conf. I). Sections of the graph enclosed by a dashed red line show force waveform peak areas for a new rubber band and used rubber pad configuration (conf. II). In case of conf. I, significantly higher force values are observed when the third, fourth and fifth roadwheels are overcoming an obstacle. The maximum force value is ≈200 kN. For all wheels, a reduction in the transmitted force to zero is observed. This is equivalent to the condition in which the roadwheels become detached from the road surface.

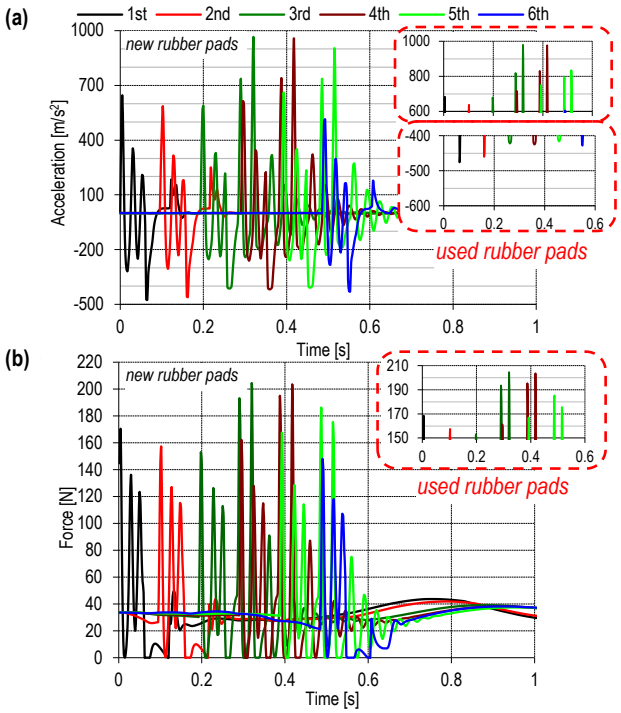

Fig. 18. Vertical acceleration waveforms of roadwheels passing a single B-type obstacle for conf. I (a) and conf. II in the section of graph enclosed by a dashed red line. Force exerted on roadwheels for conf. I (b) and conf. II in the section of graph enclosed by a dashed red line

In case of conf. II, waveform patterns are similar. The highest values of force transmission are observed for the third, fourth and sixth roadwheels, higher by an average of around 1.6%. The highest percentage increase was observed for the sixth roadwheel. The value of the force increased by 10.7%. For all roadwheels, detachment from surface was also observed. Tab. 5 summarises the detailed extreme force values and their percentages for the compared configurations.

Tab. 6 summarises data covering the maximum and minimum values of rubber deflection (for the equivalent stiffness characteristics, the determination is shown in the fourth section). Tabs. 5

and 6 confirms the detachment of all roadwheels in both scenarios. The highest deflection values are observed for the third and fourth roadwheels. In the case of the first, second and fifth roadwheels, the maximum deflection was smaller. The smallest deflection, lower by about 2 mm, was observed for the sixth roadwheel. In both configurations, detachment of roadwheels occurred. The impact of rubber pad wear on the working range (deflection) was observed for all roadwheels. Maximum deflection values decreased overall by 5.1%. The highest percentage decrease was observed for the third and fourth roadwheels.

The condition of the rubber elements has an impact on loads acting on roadwheels and its suspensions but did not significantly affect the loads acting on the vehicle hull and the driver.

Tab. 4. Roadwheel vertical acceleration peak values and relative differences for tested configurations: a new rubber pad[1] and worn-out rubber pad[2]

Roadwheel number	Acceleration [m/s²]				|Difference| [%]	
	max[1]	max[2]	min[1]	min[2]	min	max
1st	646	683	−476	−472	5.73	0.84
2nd	586	629	−461	−458	7.34	0.65
3rd	966	980	−414	−422	1.45	1.93
4th	958	977	−418	−425	1.98	1.67
5th	904	827	−408	−416	8.52	1.96
6th	513	605	−430	−428	17.9	0.47

[1]conf. I: new rubber band, new rubber pad.
[2]conf. II: new rubber band, used rubber pad

Tab. 5. Peak values and relative differences of force exerted on roadwheel for tested configurations: a new rubber pad[1] and worn-out rubber pad[2]

Roadwheel number	1st	2nd	3rd	4th	5th	6th
F_{max}[1] [kN]	161	148	202	200	188	133
F_{max}[2] [kN]	168	156	204	204	185	147
|Difference| [%]	4.43	5.48	1.47	1.87	1.34	10.7
F_{max}[1] [kN]	0*	0*	0*	0*	0*	0*
F_{max}[2] [kN]	0*	0*	0*	0*	0*	0*
|Difference| [%]	N.A.	N.A.	N.A.	N.A.	N.A.	N.A.

[1]conf. I: new rubber band, new rubber pad.
[2]conf. II: new rubber band, used rubber pad
*Detachment of the roadwheel from the ground.
N.A. – not applicable.

Tab. 6. Rubber deflection peak values and relative differences for tested configurations: a new rubber pad[1] and worn-out rubber pad[2]

Roadwheel number	Deflection [mm]				|Difference| [%]	
	min[1]	min[2]	max[1]	max[2]	min	max
1st	0*	0*	−13.4	−12.8	N.A.	4.48
2nd	0*	0*	−12.9	−12.5	N.A.	3.10
3rd	0*	0*	−14.4	−13.4	N.A.	6.94
4th	0*	0*	−14.4	−13.4	N.A.	6.94
5th	0*	0*	−13.9	−13.3	N.A.	4.32
6th	0*	0*	−12.5	−11.9	N.A.	4.80

[1]conf. I: new rubber band, new rubber pad.
[2]conf. II: new rubber band, used rubber pad
*Undeformed rubber (detachment of roadwheel from the ground).
N.A. – not applicable.

6. SUMMARY AND FINAL FINDINGS

The elasticity characteristics obtained indicate a change in the properties of rubber as a construction material. The degree of change depends on the running conditions, terrain and meteorological conditions, as well as its intensity and exposure time.

This article demonstrates that during the operation of high-speed tracked vehicles, there is intensive wear of the rubber material used in the crawler track mechanism assemblies. The shape, geometry, properties and elastic and damping characteristics change. Deterioration of the elastic damping properties of rubber elements in the suspension components does not necessarily eliminate the vehicle from further use. However, it may be one of the causes of accelerated wear of other elements or assemblies. Monitoring changes in parameters describing the properties of elements of the crawler track mechanism make it possible to build models with high accuracy corresponding to the test objects (HSTV) and to determine loads close to the real ones. As a result, it makes it possible to carry out model tests on new objects, as well as after a run undergoing modification or modernisation.

Intense wear and tear of rubber elements used in crawler track mechanisms leading to the deterioration of their elastic–damping properties indicate the relevance of further investigation of this phenomenon. This particularly concerns the durability and reliability of cover plates of crawler tracks, and load-bearing wheel counter-measurements may be suggested:

1. Selection of the shape and dimensions of the rubber elements to reduce the running resistance in rectilinear and curvilinear motions and the loads resulting from these forces.
2. Modification of the composition of the mixture from which the rubber elements of the crawler mechanism are made. This could be a direction related to the use of rubber mixtures with a graphene admixture [31].

The aforementioned measures should positively influence the technical characteristics of high-speed tracked vehicles by, for example, increasing the traction properties, reliability and durability of the internal equipment assemblies. Efforts in this direction should also have the effect of reducing vehicle maintenance and operating costs.

REFERENCES

1. Djurić R, Milis Avljević V. Investigation of the relationship between reliability of track mechanism and mineral dust content in rocks of lignite open pits. Maintenance and Reliability. 2016; 18 (1): 142-150.
2. Grygier D. The impact of operation of elastomeric track chains on the selected properties of the steel cord wires. Maintenance and Reliability. 2017; 19 (1): 95-101.
3. Dudziński P, Kosiara A, Konieczny A. Wirtualne prototypowanie nowej generacji układu jezdnego na gąsienicach elastomerowych do zastosowań arktycznych. Postępy Nauki i Techniki. 2012; 14: 64-74.
4. Czabanowski R. Numeryczna analiza obciążeń wybranych elementów podwozia z gąsienicami elastomerowymi. Przegląd Mechaniczny. 2010; nr 7-8: 30-36.
5. Dziubak T. The effects of dust extraction on multi-cyclone and non-woven fabric panel filter performance in the air filters used in special vehicles. Maintenance and Reliability. 2016; 18 (3): 348-357.
6. Gniłka J, Mężyk A. Experimental identification and selection of dynamic properties of a high-speed tracked vehicle suspension system. Maintenance and Reliability. 2017; vol. 19 (1): 108-113.
7. Bogucki R. Badania prototypów nakładek elastomerowych na człony taśm gąsienicowych. Szybkobieżne Pojazdy Gąsienicowe. 2013; 1 (32): 37-46.

8. Rybak P. Tracked or Wheeled Chassis. Journal of Kones Powertrain and Transport. 2007; 14 (3):527-536.
9. Rybak P. Operating loads of impulse nature acting on the special equipment of the combat vehicles. Maintenance and Reliability. 2014; 16 (3): 347-353.
10. Campanelli M, Shabana AA, Choi JH. Chain vibration and dynamic stress in three-dimensional multibody tracked vehicles. Multibody System Dynamics. 1998; 2**:** 277–316.
11. Lee K. A numerical method for dynamic analysis of tracked vehicles of high mobility. KSME International Journal. 2000; 14 (10): 1028-1040.
12. Ma ZD, Perkins NC. A super-element of track-wheel-terrain interaction for dynamic simulation of tracked vehicles. Multibody System Dynamics. 2006; 15: 351–372.
13. Wallin M, Aboubakr AK, Jayakumar P,·Letherwood MD,·Gorsich DJ,·Hamed A,·Shaban A. A comparative study of joint formulations: application to multibody system tracked vehicles. Nonlinear Dynamics. 2013; 74 (3): 783–800.
14. Wang P, Rui X, Yu H. Study on dynamic track tension control for high-speed tracked vehicles. Mechanical Systems and Signal Processing. 2019; 132: 277-292. Available from: doi.org/10.1016/j.ymssp.2019.06.031
15. Wang Z, Lv H, Zhou X, Chen Z, Yang Y. Design and Modeling of a Test Bench for Dual-Motor Electric Drive Tracked Vehicles Based on a Dynamic Load Emulation Method. Sensor. 2018; 18: 1-20.
16. Dudziński P, Chołodowski J. A method for predicting the internal motion resistance of rubber-tracked undercarriages, Pt. 1. A review of the state-of-the-art methods for modeling the internal resistance of tracked vehicles. Journal of Terramechanics. 2021; 96: 81-100. Available from: doi.org/10.1016/j.jterra.2021.02.006
17. Chołodowski J, Dudziński P, Ketting M. A method for predicting the internal motion resistance of rubber-tracked undercarriages, Pt. 3. A research on bending resistance of rubber tracks. Journal of Terramechanics. 2021; 97: 71-103. Available from: https://doi.org/10.1016/j.jterra.2021.02.005
18. Liu W, Cheng K, Wang J. Failure analysis of the rubber track of a tracked transporter. Advances in Mechanical Engineering. 2018; 10 (7): 1–8.
19. Gat G, Franco Y, Shmulevich I. Fast dynamic modeling for off-road track vehicles. Journal of Terramechanics. 2020; 92: 1-12. Available from: doi: 10.1016/j.jterra.2020.09.001.
20. Burdziński Z. Teoria ruchu pojazdu gąsienicowego. Warszawa: WKŁ; 1972.
21. Mahalingam I, Padmanabhan C. A novel alternate multibody model for the longitudinal and ride dynamics of a tracked vehicle. Vehicle System Dynamics. 2021; 59(3): 433-457.
22. Edwin P, Shankar K, Kannan K. Soft soil track interaction modeling in single rigid body tracked vehicle models. J Terramechanics. 2018; 77:1-14.
23. Sandu C, Freeman JS. Military tracked vehicle model. Part I: Multibody dynamics formulation.Int J Veh Syst Model Test. 2005; 1(1-3):48–67.
24. Janarthanan B, Padmanabhan C, Sujatha C. Longitudinal dynamics of a tracked vehicle:simulation and experiment. J Terramechanics. 2012;49(2):63-72.
25. Nabagło T, Jurkiewicz A, Kowal J. Modeling verification of an advanced torsional spring for tracked vehicle suspension in 2S1 vehicle model. Engineering Structures. 2021; 229: 111623.
26. Ata WG, Oyadiji SO. An investigation into the effect of suspension configurations on the performance of tracked vehicles traversing bump terrains. Vehicle System Dynamics. 2014; 52(7): 1-25.
27. Sandu C, Freeman JS. Military tracked vehicle model. Part II: Case study. Int J Veh Syst Model Test. 2005;1(1-3):216-231.
28. Budynas R, Nisbett K. Shigley's Mechanical Engineering Design. McGraw Hill Education; 2019.
29. Borkowski W, Rybak P, Hryciów Z. Modele częściowe w analizie obciążeń struktur nośnych wozów bojowych. Biuletyn Wojskowej Akademii Technicznej. 2006; 55(4):221-232.
30. Hryciów Z; Małachowski J; Rybak P, Wiśniewski A. Research of Vibrations of an armoured Personnel Carrier Hull with FE Implementation. Materials. 2021; 14,6807:1-18. Available from: doi.org/10.3390/ma14226807.
31. Hebda M, Łopata A. Grafen – materiał przyszłości. Czasopismo Techniczne. Mechanika. 2012; R. 109, Z. 22, 8-M: 45-53.

Piotr Rybak: https://orcid.org/0000-0002-7063-9913

Zdzisław Hryciów: https://orcid.org/0000-0002-6281-1883

Bogusław Michałowski: https://orcid.org/0000-0002-5793-2744

Andrzej Wiśniewski: https://orcid.org/0000-0002-2089-1942